

# Measurement of the $\Gamma(K^+ \rightarrow e^+ \nu)/\Gamma(K^+ \rightarrow \mu^+ \nu)$ branching ratio using stopped positive kaons at J-PARC

---

**Suguru Shimizu\*** for the J-PARC E36 collaboration

*Department of physics, Osaka University*

*1-1 Machikaneyamacho, Toyonaka city, Osaka, Japan*

*E-mail: suguru@phys.sci.osaka-u.ac.jp*

The J-PARC E36 experiment is aiming at searching for the lepton universality violation by precisely measuring the ratio of the branching ratio of the  $K^+ \rightarrow e^+ \nu$  ( $K_{e2}$ ) to  $K^+ \rightarrow \mu^+ \nu$  ( $K_{\mu2}$ ) decays. The E36 experiment was performed at J-PARC employing a stopped  $K^+$  beam in conjunction with a 12-sector iron-core superconducting toroidal spectrometer. Charged particle momenta were calculated by reconstructing the tracks in the spectrometer. Particle discrimination between  $e^+$  and  $\mu^+$  was carried out using an aerogel Cherenkov counters and a lead-glass Cherenkov counter, as well as by measuring the time-of-flight between TOF counters. The peak structure due to the  $K_{e2}$  decays was successfully observed in the  $e^+$  momentum spectrum. The structure-dependent radiative  $K^+ \rightarrow e^+ \nu \gamma$  ( $K_{e2\gamma}$ ) events can be selected by requiring one photon hit in the CsI(Tl) calorimeter. The experimental spectra were reproduced by the Monte Carlo simulation, which indicates a correct understanding of the experimental conditions.

*XIV International Conference on Heavy Quarks and Leptons (HQL2018)*

*May 27- June 1, 2018*

*Yamagata Terrsa, Yamagata, Japan*

---

\*Speaker.

## 1. Introduction

High precision electroweak tests represent a powerful tool to check the Standard Model (SM) and to obtain indirect hints of new physics. The  $K^+ \rightarrow l^+ \nu$  ( $K_{l2}$ ), which is the simplest semi-leptonic decay among the  $K^+$  decay channels, is one of the best channels to perform such tests. Lepton universality, which can be expressed as the identical coupling constants of the three lepton generations, the electron, muon, and tau, is a basic assumption in the SM. Violation of lepton universality clearly indicates the existence of new physics beyond the SM. The  $K_{l2}$  hadronic form factor can be canceled out by forming the ratio of the electric ( $K_{e2}$ ) and muonic ( $K_{\mu2}$ ) decay channels with radiative correction ( $\delta_r$ ) as,

$$R_K^{\text{SM}} = \frac{\Gamma(K^+ \rightarrow e^+ \nu)}{\Gamma(K^+ \rightarrow \mu^+ \nu)} = \frac{m_e^2}{m_\mu^2} \cdot \left( \frac{m_K^2 - m_e^2}{m_K^2 - m_\mu^2} \right)^2 \cdot (1 + \delta_r) \quad (1.1)$$

under the assumption of  $\mu$ - $e$  universality. The factor  $(m_e/m_\mu)^2$  accounts for the helicity suppression of  $K_{e2}$  decay due to the  $V - A$  structure of the charged weak current, and in other words, enhances the sensitivity to effects beyond the SM. As a result, the SM prediction of  $R_K^{\text{SM}}$  is determined to be  $(2.477 \pm 0.001) \times 10^{-5}$  with excellent accuracy and this makes it possible to search for new physics effects by a precise  $R_K$  measurement [1].

Recently, the NA62 [2] and KLOE [3] groups reported the experimental results of the  $R_K$  measurement. In the NA62 measurement, an in-flight kaon beam with particle momentum from 15 to 65 GeV/c, was used, where  $K_{\mu2}$  and structure-dependent radiative  $K^+ \rightarrow e^+ \nu \gamma$  ( $K_{e2\gamma}$ ) decays were the main background sources in the  $K_{e2}$  sample. The treatment of these backgrounds was one of the most difficult points to determine the  $R_K$  value in the NA62 experiment. Since low energy kaons from  $\phi \rightarrow K^+ K^-$  were used in the KLOE experiment, the kinematical resolution of  $K_{l2}$  decays was better than that in NA62. However, the experimental result was dominated by the statistical uncertainty because of low-intensity of the kaon beam. The NA62 and KLOE results were obtained to be

$$R_K = (2.488 \pm 0.007 \pm 0.007) \times 10^{-5} (\text{NA62}), \quad (1.2)$$

$$R_K = (2.493 \pm 0.025 \pm 0.019) \times 10^{-5} (\text{KLOE}). \quad (1.3)$$

The combined value was determined by calculating the error-weighted average as,

$$R_K = (2.488 \pm 0.009) \times 10^{-5} \quad (1.4)$$

which is consistent with the SM within the error. Since the experimental error is about 10 times larger than the theoretical one, there is still room for further improvement of the  $R_K$  determination.

## 2. The J-PARC E36 experiment

The E36 experiment was performed in 2015 at J-PARC employing a stopped  $K^+$  beam in conjunction with a 12-sector iron-core superconducting toroidal spectrometer [4]. Schematic cross sectional side and end views of the detector configuration are shown in Fig. 1. The  $K_{e2}$  ( $P_{e^+}=247$  MeV/c) and  $K_{\mu2}$  ( $P_{\mu^+}=236$  MeV/c) events were accepted by analyzing the charged particle momentum using this magnetic spectrometer. Details of the setup are well documented in Ref. [4].

In order to compare the experimental  $R_K$  with the SM prediction, the internal bremsstrahlung (IB) process in the radiative  $K^+ \rightarrow e^+ \nu \gamma$  and  $K^+ \rightarrow \mu^+ \nu \gamma$  decay has to be included in the  $K_{e2}$  and  $K_{\mu2}$  samples, respectively. On the other hand, the structure-dependent (SD) radiative  $K^+ \rightarrow l^+ \nu \gamma$  decays [3] are backgrounds and have to be subtracted from the observed  $K_{e2}$  and  $K_{\mu2}$  samples in the analysis. The radiated photons from the above structure dependent processes were measured by a CsI(Tl) calorimeter, as shown in Fig. 1.

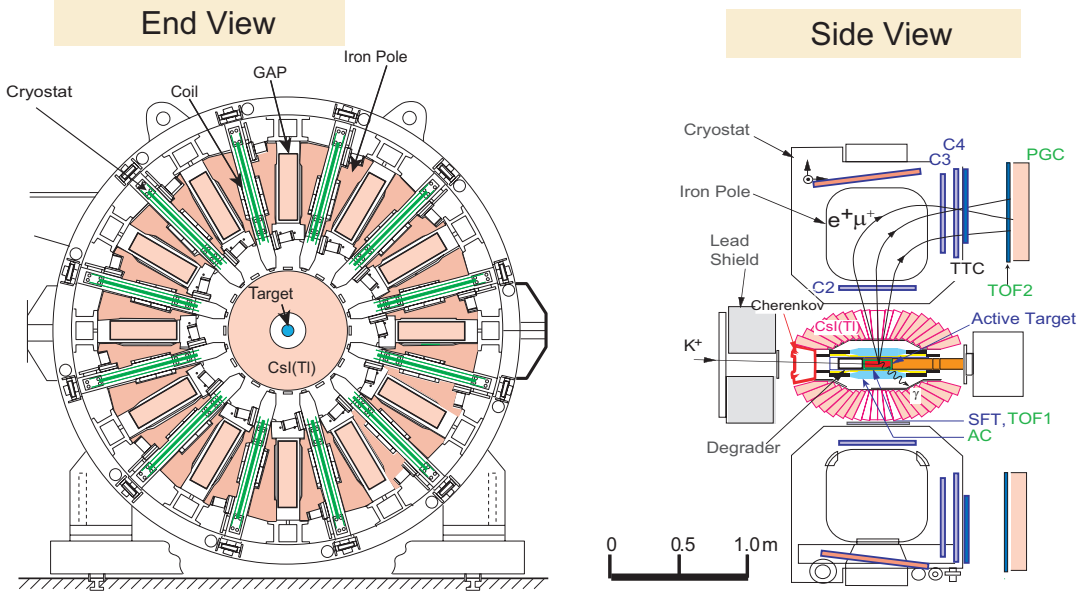


**Figure 1:** Schematic cross sectional side and end views of the E36 detector configuration. Particle identification was carried out using an aerogel Cherenkov counters and a lead-glass Cherenkov counter, and by measuring the time-of-flight between the TOF1 and TOF2 scintillating counters. The photon energy and hit position were measured by the CsT(Tl) calorimeter.

A separated 760-MeV/ $c$  beam was extracted using the J-PARC K1.1BR beamline. The beam was slowed down by a BeO degrader and stopped in a position sensitive fiber target. Charged particles from the target were tracked using a spiral-fiber tracker (SFT) [5] surrounding the  $K^+$  stopper and three multi-wire proportional chambers (C2, C3, C4) in each spectrometer sector [6]. The C2 and C3/C4 chambers were located at the entrance and exit of the magnet gaps, respectively. The  $K_{e2}$  and  $K_{\mu2}$ , and their radiative decays are collected with a central magnetic field of the spectrometer,  $B=1.5$  T. In order to remove  $K^+ \rightarrow \pi^0 e^+ \nu$  ( $K_{e3}$ ) and  $K^+ \rightarrow \pi^0 \mu^+ \nu$  ( $K_{\mu3}$ ) backgrounds, the  $K_{e2}$  and  $K_{\mu2}$  events were identified by requiring the  $e^+$  and  $\mu^+$  momentum to be higher than the  $K_{e3}$  and  $K_{\mu3}$  endpoints ( $P_e^{\max}=228$  MeV/ $c$ ,  $P_\mu^{\max}=215$  MeV/ $c$ ). Particle discrimination between  $e^+$  and  $\mu^+$  was carried out using an aerogel Cherenkov counters [7] and a lead-glass Cherenkov counters [8], and by measuring the time-of-flight between the TOF1 and TOF2 scintillating counters. The TOF1 counters surround the fiber target and TOF2 was located about 90 cm behind C4. The photon detector, an assembly of 768 CsI(Tl) crystals, covers 70% of the total solid angle [6, 9]. Since photons produce electro-magnetic showers, their energy was shared among several crystals. The photon energy and hit position were obtained by summing the energy deposits and by determining the energy-weighted centroid, respectively. After selecting the  $e^+$  events, due to the finite

acceptance of the CsI(Tl) calorimeter, the  $K_{e2}$ ,  $K_{e2\gamma}$ , and  $K_{e3}$  decays could be accepted as the  $0\gamma$  event sample, while the  $K_{e2\gamma}$  and  $K_{e3}$  decays only contributed to the  $1\gamma$  sample.

### 3. Data analysis

#### 3.1 Overview of the analysis

The number of the accepted  $K_{e2}$  ( $N(K_{e2})$ ) and  $K_{\mu2}$  ( $N(K_{\mu2})$ ) events after background subtraction can be described as,

$$N(K_{e2}) = N_K \times \Omega(K_{e2}) \times \text{Br}(K_{e2}), \quad (3.1)$$

$$N(K_{\mu2}) = N_K \times \Omega(K_{\mu2}) \times \text{Br}(K_{\mu2}). \quad (3.2)$$

Here  $N_K$  is the number of stopped kaons in the target, Br is the branching ratio, and  $\Omega$  is the detector acceptance. Therefore, the  $R_K = \Gamma(K_{e2})/\Gamma(K_{\mu2})$  ratio can be obtained by calculating ratio of the accepted  $K_{e2}$  and  $K_{\mu2}$  event numbers corrected for the detector acceptance as

$$R_K = \Gamma(K_{e2})/\Gamma(K_{\mu2}) = \text{Br}(K_{e2})/\text{Br}(K_{\mu2}) \quad (3.3)$$

$$= N(K_{e2})/N(K_{\mu2}) \cdot \Omega(K_{\mu2})/\Omega(K_{e2}). \quad (3.4)$$

The detector acceptance was calculated by Monte Carlo simulation. It should be noted that the analysis procedure is identical between  $K_{e2}$  and  $K_{\mu2}$  except for the particle identification in order to reduce the systematic uncertainty due to the analysis.

#### 3.2 $K_{e2}$ and $K_{e2\gamma}$ event selections

The charged particle momentum in the spectrometer gap was calculated by reconstructing the track using the active target, SFT, C2, C3, and C4, as shown in Fig. 2(a). Then, the original momentum was determined by correcting for the energy loss in the target, as shown in Fig. 2(b). Events from particle decays in-flight and scattering of the particles from the magnet pole faces were eliminated by removing large tracking- $\chi^2$  events. Monochromatic peaks due to the  $K_{\mu2}$  and  $K^+ \rightarrow \pi^+ \pi^0$  ( $K_{\pi2}$ ) decays are clearly observed in the figure, although the  $K_{e2}$  events are not seen. Next, choosing  $e^+$  particles using the three PID detectors, the peak structure due to the genuine  $K_{e2}$  decays are successfully observed in the  $e^+$  momentum spectrum, as shown in Fig. 3. The black histogram is the experimental data which includes the  $K_{e2\gamma}$  and  $K_{e3}$  backgrounds as well as the  $K_{e2}$  events. It should be noted that these spectra were obtained using a small fraction of the whole E36 data set and the PID selection conditions are not yet optimized in the current analysis stage.

Since the SD radiative  $K_{e2\gamma}$  process is a serious background for the  $R_K$  measurement, the characteristics of this decay channel have to be well understood for the background subtraction. In order to study the SD radiative  $K_{e2\gamma}$  decay, events with one photon cluster in the CsI(Tl) calorimeter generated by a radiative photon were selected to pick up these events from the above accepted  $e^+$  events. The squared missing mass ( $M_{\text{miss}}^2$ ) defined as,

$$M_{\text{miss}}^2 = (M_K - E_{e^+} - E_\gamma)^2 - (\vec{P}_{e^+} + \vec{P}_\gamma)^2, \quad (3.5)$$

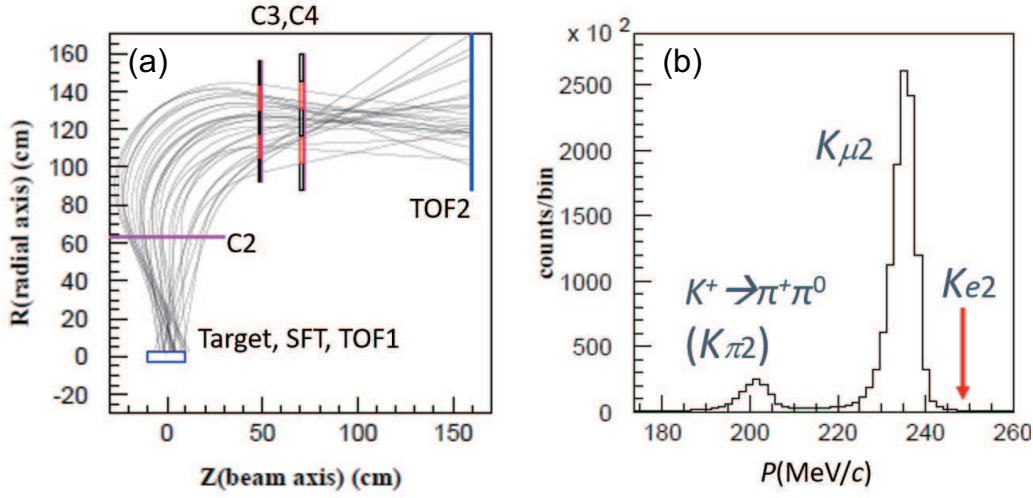


**Figure 2:** (a) Reconstructed charged particle tracks using active target, SFT, C2, C3, and C4. (b) Momentum spectrum corrected for the energy loss in the target. Monochromatic peaks due to the  $K_{\mu 2}$  and  $K_{\pi 2}$  decays are clearly seen.

where  $E$  and  $\vec{P}$  are the energy and momentum vector, respectively, was required to be  $-8000 < M_{\text{miss}}^2 < 5000$  ( $\text{MeV}/c^2$ )<sup>2</sup> to remove accidental backgrounds in the CsI(Tl) calorimeter. The experimental SD  $K_{e2\gamma}$  events were successfully extracted with the present selection conditions. They are shown in Fig. 4 for (a)  $P_{e^+}$ , (b)  $E_{\gamma}$ , (c)  $(e^+, \gamma)$  opening angle, and (d)  $M_{\text{miss}}^2$ . The dots are the experimental data and the histograms are the simulation results. The  $K_{e2\gamma}$  form factors will be obtained by comparing the experimental data with the simulation, and the background fraction in the  $K_{e2}$  sample will be determined using the  $K_{e2}$  form factors.

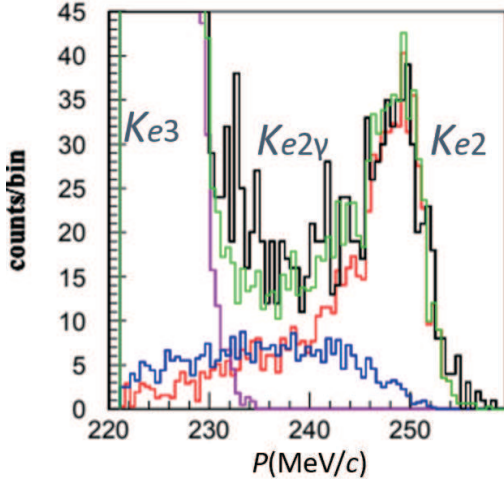


**Figure 3:** Positron momentum spectrum obtained by using three PID detector information. Black histogram is the experimental data. Red, blue, and purple histograms are the Monte Carlo simulation assuming the  $K_{e2}$ , SD radiative  $K_{e2\gamma}$ , and  $K_{e3}$  decays, respectively. Green one is sum of the three MC processes.

In the current Monte Carlo (MC) simulation based on a GEANT4 code, the  $K_{e2\gamma}$  data were

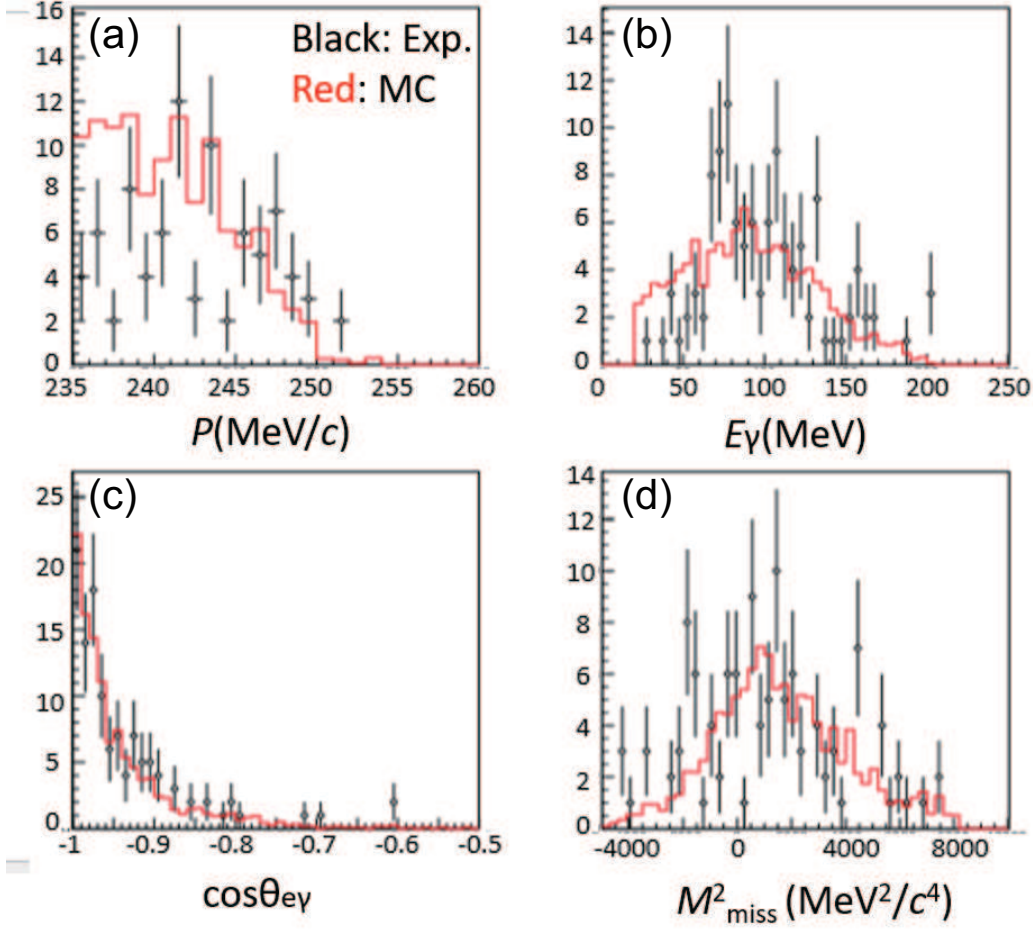


**Figure 4:** Dots are the experimental  $K_{e2\gamma}$  events identified with the present selection conditions for (a)  $P_{e^+}$ , (b)  $E_\gamma$ , (c)  $(e^+, \gamma)$  opening angle, (d)  $M_{\text{miss}}^2$ . Histograms are the simulation results.

generated according to the matrix elements given in Ref. [10] and the form factors obtained by the KLOE group [3] was adopted. Here, only the SD process was taken into account because the present result is not sensitive to enough to study the IB contribution. The red, blue, and purple histograms in Fig. 3 are the MC simulations of  $K_{e2}$ ,  $K_{e2\gamma}$ , and  $K_{e3}$  decays. The experimental data are consistent with the MC simulation.

### 3.3 Summary

The J-PARC E36 experiment is aiming at searching for the lepton universality violation by precisely measuring the ratio of the decay widths of the  $K^+ \rightarrow e^+ \nu$  and  $K^+ \rightarrow \mu^+ \nu$  decays. The E36 experiment was performed at J-PARC employing a stopped  $K^+$  beam in conjunction with a 12-sector iron-core superconducting toroidal spectrometer. Particle discrimination between  $e^+$  and  $\mu^+$  was carried out using an aerogel Cherenkov counters and a lead-glass Cherenkov counter, as well as by measuring the time-of-flight between the TOF1 and TOF2 scintillating counters. The peak structure due to the  $K_{e2}$  decays was successfully observed in the  $e^+$  momentum spectrum. Also, the SD radiative  $K_{e2\gamma}$  events can be selected by requiring one photon hit in the CsI(Tl) calorimeter. The

experimental spectra were reproduced by the Monte Carlo simulation, which indicates a correct understanding of the experimental conditions. The analysis is still in progress and the final  $R_K$  result will be reported soon.

## References

- [1] V. Cirigliano et al., Phys. Rev. Lett. **99** (2007) 231801.
- [2] C. Lazzeroni et al., Phys. Lett. **B719** (2013) 326-336.
- [3] F. Ambrosino et al., Eur. Phys. J. **C64** (2009) 627; Erratum-ibid. **C65** (2010) 703.
- [4] E36 experimental proposal, TREK homepage, <http://trek.kek.jp/>
- [5] O. Mineev et al., Nucl. Instrum. Meth. **A847** (2017) 136-141.
- [6] M. Abe et al., Nucl. Instrum. Meth. **A506** (2003) 60-91.
- [7] M. Tabata et al., Nucl. Instrum. Meth. **A795** (2015) 206-212.
- [8] Y. Miyazaki et al., Nucl. Instrum. Meth. **A779** (2015) 13-17.
- [9] H. Ito et al., Nucl. Instrum. Meth. **A901** (2018) 1-5.
- [10] J. Bijnens et al., Nucl. Phys. **B396** (1993) 81; J. Bijnens et al., in The Second DAPHNE Physics Handbook, <http://www.Inf.infn.it/theory/dafne.html>.